PNAS
www.pnas.org

Supplementary Information for:
Interleukin-6 mediates PSAT1 expression and serine metabolism in TSC2-deficient cells

Ji Wang[1*], Harilaos Filippakis[1*], Thomas Hougard[1], Heng Du[1], Chenyang Ye[2], Heng-Jia Liu[1], Long Zhang[1], Khadijah Hindi[1], Shefali Bagwe[1], Julie Nijmeh[1], John M. Asara[3], Wei Shi[4], Souheil El-Chemaly[1], Elizabeth P. Henske[1#], Hilaire C. Lam[1#]

[1]Pulmonary and Critical Care Medicine, Brigham and Women's Hospital, Harvard Medical School, Boston, MA 02115
[2]The F.M. Kirby Neurobiology Center, Boston Children's Hospital, Department of Neurology, Harvard Medical School, Boston, MA 02115
[3]Division of Signal Transduction, Beth Israel Deaconess Medical Center and Department of Medicine, Harvard Medical School Boston, MA, USA 02215
[4]Department of Surgery, Children's Hospital Los Angeles, Keck School of Medicine, University of Southern California, Los Angeles, CA 90027

Hilaire C. Lam
Email: hclam@bwh.harvard.edu

Elizabeth P. Henske
Email: ehenske@bwh.harvard.edu

This PDF file includes:

Supplementary Information Text

Materials and Methods

Cell lines and treatment

The inducible raptor and rictor knockout MEFs were generated in the laboratory of Michael Hall, the cells were cultured in 10% FBS in DMEM and treated with 1uM of tamoxifen or ethanol control for 72 h to induce knockout prior to harvest (40).

For IL-6 knockout, TSC2-deficient cells were transduced with single lentivirus containing an spCas9 and sgRNA (CTTCCCTACTTCACAAGTC) expression cassette to target spCas9 cleavage to IL-6. The lentiviral plasmids (LV01) and lentivirus production were obtained from Sigma-Aldrich. Cells were sorted for GFP expression by flow cytometry and maintained in puromycin (3μg/mL). IL-6 knockout was confirmed by Sanger sequencing and ELISA. For PSAT1 overexpression, lentiviral vector of PSAT1 (EX-Mm13089-Lv197-GS, GeneCopoeia) was transfected into HEK-293T cells along with lentiviral packaging mix to produce lentivirus. Tsc2-deficient cells with or without IL-6 overexpression were transfected with lentivirus and selected with blasticidin at 10μg/ml. Knockdown experiments were performed using Silencer Select siRNA from Ambion STAT3 (4392420) and IL-6RAa (4390771) transfected using Lipofectamine RNAiMax Reagent (Invitrogen).

All cells tested negative for mycoplasma contamination using MycoAlert (Lonza) and were re-tested monthly. Cells were cultured at 37°C in 5% CO2 in DMEM supplemented with 10% FBS and gentamycin sulfate (50μg/mL). For serum-free conditions, cells were cultured in DMEM without serum.

Cytokine Array. *A* RayBiotech Human Cytokine Array 5 was used to detect differential secretion of cytokines from angiomyolipoma-derived 621-101 cells compared to human embryonic kidney

HEK293 cells according to the manufacturer's instructions. Cells were grown in IIA Complete Media and serum starved overnight (16h) in 3ml of media on 10cm dishes. One mL of media was applied to the cytokine array and incubated for 2 hours. As a control, one array was incubated with unconditioned media.

***ELISA*.** ELISA was performed using conditioned media (~80% confluent cells, concentrated with Millipore UFC 900324 filters) and normalized by protein concentration (Bio-Rad Laboratories, #5000006). Levels of secreted IL-6 were determined according to the manufacturer's protocol (R&D Systems, IL-6 Quantikine ELISA Kit).

Crystal violet assay. Cells were seeded at a density of 1,000 cells/well in 96-well plates and changed into serum-free media after 24 hours. At the indicated time points, cells were fixed for 15 minutes with 10% formalin and then stained with 0.5% crystal violet in distilled water for 20 minutes. Crystal violet was removed and cells were washed with water followed by drying at room temperature. Crystal violet was solubilized with 200 ml of methanol and measured with a plate reader (OD 540; BioTek, Winooski, VT, USA). Proliferation was assessed by comparing the change in OD 540 at 24, 48 and 72 h as normalized to 0h (start of serum-free proliferation) for each cell line.

Transwell migration assay. Migration was evaluated as described previously (1). Briefly $5x10^4$ cells were seeded in 100 μl of serum-free DMEM in the upper chamber of a 6.5 mm polycarbonate Transwell with 8.0 μm pores (Corning, USA), through which the cells were allowed to migrate for 6 h at 37 °C toward 10% FBS in the basal compartment. At the end of the incubation, migrated cells on the lower surface of the transwell were fixed, stained, and quantified.

Soft agar assay. Soft agar assays were performed to measure anchorage-independent growth. Briefly, 5×10^3 cells were placed into a single well in a 6-well plate. Cells were embedded into

0.4% low-melting agarose (Sigma) and layered on top of a 0.8% agarose base. After 2 weeks of growth, the cells were fixed and analyzed. Colony number was quantitated using ImageJ (v1.53).

Wound healing assay. Cells were seeded into six-well plates in DMEM culture medium and allowed to grow for 24 hours until confluency was reached. Cells were then washed with 1x PBS, and a scratch was made using a 200 µl tip at the center of the well. The monolayers were imaged at the indicated times using a light microscope at 100x magnification. The results were quantified using ImageJ (v1.53) software.

RNA extraction and quantitative real-time PCR. Total RNA was extracted using RNeasy Mini Kit (QIAGEN, USA). The RNA concentration was measured using a Nanodrop 2000c (Thermo Scientific, USA). Two micrograms of RNA were reverse transcribed using a High-Capacity cDNA Reverse Transcription Kit (Thermofisher, USA) with random primers. For qPCR, a Taqman-based method was used and the relative quantitation of gene expression was determined using the comparative CT (ΔΔCT) method and normalized to β-actin gene and a calibrator sample that was run on the same plate. PCR primers and probe sets were obtained from Thermofisher, USA: IL-6 (assay ID Mm00446191_m1, 124 bp amplicon length), PSAT1 (assay ID Mm04932904_m1, 109 bp amplicon length), and β-actin control (cat# 4351315).

Western blot analysis. After indicated treatment, live cells were lysed on ice in 1× RIPA (Cell Signaling Technology) containing phosphatase and protease inhibitors. For the membrane fractionation experiments Mem-PER™ Plus Membrane Protein Extraction Kit was used according to manufacturer's instructions (Thermo Scientific, 89842). The concentration of proteins was determined using a Bio-Rad Protein Assay Dye Reagent Concentrate (Bio-Rad Laboratories, #5000006). A total of 15 µg of protein from each sample were mixed with NuPAGE™ LDS Sample Buffer (Thermofisher, NP0007) and Reducing Sample Buffer (Invitrogen, NP009, USA), resolved on a 4-12% Bis-Tris gels (Thermofisher), then transferred to PVDF membranes

(MilliporeSigma, USA). Blots were blocked with 5% milk and incubated with primary and second antibodies. Chemiluminescence was captured with Syngene G-Box gel documentation system.

Immunohistochemistry staining. Kidneys were formalin-fixed, paraffin-embedded, and tissue was cut in 3- to 4-μm sections then air-dried overnight. The sections were deparaffinized, rehydrated, and subjected to heat-induced epitope retrieval using low pH target retrieval solution for 15 minutes. Sections were incubated with Ki67 of PSAT1 primary antibody (1:100 dilution). Slides were developed using DAB and counterstained with hematoxylin.

Targeted Mass Spectrometry. Samples were re-suspended using 20 mL HPLC grade water for mass spectrometry. 5-7 μL were injected and analyzed using a hybrid 6500 QTRAP triple quadrupole mass spectrometer (AB/SCIEX) coupled to a Prominence UFLC HPLC system (Shimadzu) via selected reaction monitoring (SRM) of a total of 270 endogenous water-soluble metabolites for steady-state analyses of samples. Some metabolites were targeted in both positive and negative ion mode for a total of 305 SRM transitions using positive/negative ion polarity switching. ESI voltage was +4950V in positive ion mode and –4500V in negative ion mode. The dwell time was 3 ms per SRM transition and the total cycle time was 1.39 seconds. Approximately 10-14 data points were acquired per detected metabolite. Samples were delivered to the mass spectrometer via hydrophilic interaction chromatography (HILIC) using a 4.6 mm i.d x 10 cm Amide XBridge column (Waters) at 400 μL/min. Gradients were run starting from 85% buffer B (HPLC grade acetonitrile) to 42% B from 0-5 minutes; 42% B to 0% B from 5-16 minutes; 0% B was held from 16-24 minutes; 0% B to 85% B from 24-25 minutes; 85% B was held for 7 minutes to re-equilibrate the column. Buffer A was comprised of 20 mM ammonium hydroxide/20 mM ammonium acetate (pH=9.0) in 95:5 water:acetonitrile. Peak areas from the total ion current for each metabolite SRM transition were integrated using MultiQuant v3.0 software (AB/SCIEX) (2, 3).

Analysis of metabolomics data including the generation of heatmaps and metabolite set enrichment analysis (MSEA) was performed using the open access MetaboAnalyst Software (v4.0 or 5.0).

Animal Studies

Intraperitoneal injection was done with 200 ug of αIL-6 antibody or control rat IgG antibody (Bioxcell) three times per week as previously described (57). After a total of 4 weeks of treatment, mice were harvested and the severity of renal lesions was scored using previously established macroscopic and microscopic scoring methods (43, 76).

Macroscopic cysts per kidney were scored according to size: < 1mm, score 1; 1–1.5, score 2; 1.5–2, score 5; and > 2, score 10. The sum of the cyst scores were determined and reported per kidney. Microscopic kidney tumor scores were determined by an observer blinded to the experimental conditions using a semi-quantitative algorithm and hematoxylin and eosin (H&E) sections of samples prepared by embedding 1 mm-interval sections. Each tumor or cyst identified was measured (length, width) and percent of the lumen filled by tumor determined (0% for a simple cyst, and 100% for a completely filled, solid tumor). The measurements were converted into a score using a previously established formula(43).

Semi-quantitative analysis of PSAT1 immunohistochemistry was performed by a blinded observer who scored the PSAT1 signal on a sale from 0-5 (0-no signal, 5-maximum observed signal) in ~10 renal lesions per mouse. The average score for each mouse was then calculated and the Log2 fold change of the aIL-6 antibody treated mice was calculated relative to the IgG control mice.

A

	A	B	C	D	E	F	G	H	I	J	K
1	POS	POS	POS	POS	NEG	NEG	ENA-78 (CXCL5)	G-CSF	GM-CSF	GRO a/b/g	GRO alpha (CXCL1)
2	I-309 (CCL1)	IL-1 alpha (IL-1 F1)	IL-1 beta (IL-1 F2)	IL-2	IL-3	IL-4	IL-5	IL-6	IL-7	IL-8 (CXCL8)	IL-10
3	IL-12 p40/p70	IL-13	IL-15	IFN-gamma	MCP-1 (CCL2)	MCP-2 (CCL8)	MCP3 (CCL7)	M-CSF	MDC (CCL22)	MIG (CXCL9)	MIP-1 beta (CCL4)
4	MIP-1 delta (CCL15)	RANTES (CCL5)	SCF	SDF-1 alpha	TARC (CCL17)	TGF beta 1	TNF alpha	TNF beta (TNSF1B)	EGF	IGF-1	Angiogenin
5	OSM	TPO	VEGF-A	PDGF-BB	Leptin	BDNF	BLC (CXCL13)	Ck beta 8-1 (CCL23)	Eotaxin-1 (CCL11)	Eotaxin-2 (CCL24)	Eotaxin-3 (CCL26)
6	FGF-4	FGF-6	FGF-7 (KGF)	FGF-9	FLT-3 Ligand	Fractalkine (CX3CL1)	GCP-2 (CXCL6)	GDNF	HGF	IGFBP-1	IGFBP-2
7	IGFBP-3	IGFBP-4	IL-16	IP-10 (CXCL10)	LIF	LIGHT (TNFSF14)	MCP-4 (CCL13)	MIF	MIP-3 alpha (CCL20)	NAP-2 (CXCL7)	NT-3
8	NT-4	OPN (SPP1)	OPG (TNFRSF11B)	PARC	PLGF	TGF beta2	TGF beta3	TIMP-1	TIMP-2	POS	POS

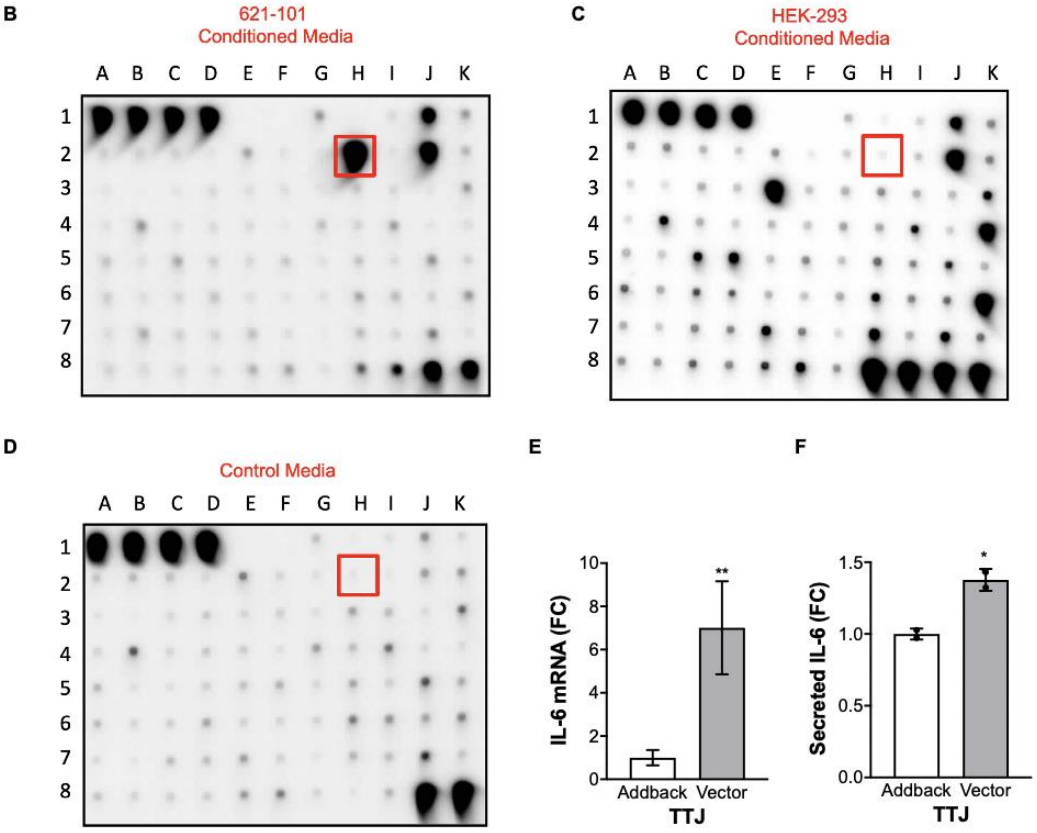

Fig. S1. Increased IL-6 secretion in conditioned media from TSC2-deficient cells. (*A*) Layout of cytokine positions in RayBiotech Human Cytokine Array 5. (*B*) Cytokine array showing IL-6 expression is elevated in conditioned media from TSC2-deficient, patient-derived angiomyolipoma cells (621-101). (*C*) Cytokine array showing IL-6 expression in conditioned media from human embryonic kidney HEK293 cells. (*D*) Media incubated without cells was used as a blank control for the cytokine profile. (*E*) *IL-6* mRNA expression is increased in TSC2-deficient TTJ cells compared to TSC2 addback cells. (*F*) Secreted IL-6 is increased in conditioned media from TSC2-deficient TTJ cells compared to TSC2 addback cells.

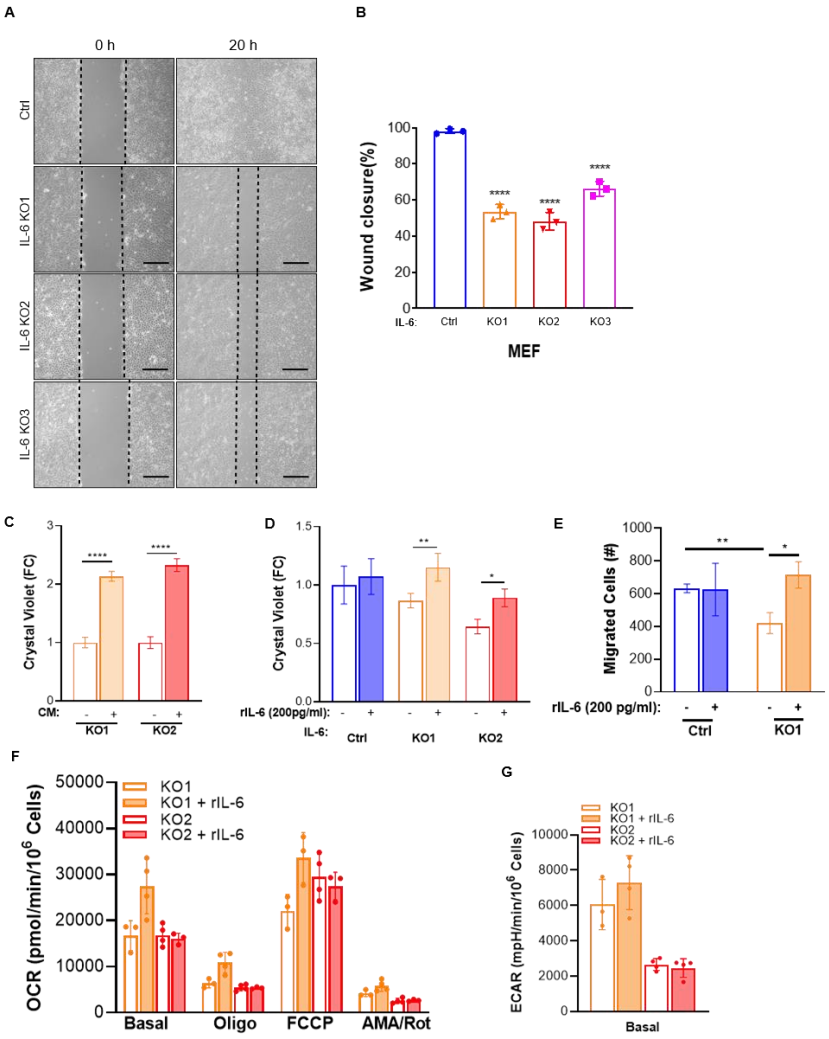

Fig. S2. Rescue of IL-6 knockout cell proliferation, migration and bioenergetic assays. (*A*) IL-6 knockout using three separate CRISPR/Cas9 clones shows decreased wound closure compared to control cells. (*B*) Quantification of percent area filled between the two leading edges at 20 h compared to 0 h (0% filled). (C) The proliferation at 96h of IL-6 knockout, TSC2 deficient cells was rescued by conditioned media was generated by concentrating serum free media from TSC2 deficient cells at 24 hours. (D) The proliferation at 72h of IL-6 knockout, TSC2 deficient cells was rescued by rIL-6 (200pg/ml) treatment in serum free conditions. (E) rIL-6 rescued transwell migration of, IL-6 knockout cells. Cells were pre-treated with rIL-6 (24h, 200pg/ml) and then seeded into the apical side of the transwell with rIL-6 or not treated controls. *F*) OCR and (*G*) ECAR are unchanged in IL-6 KO cells upon treatment with rIL-6. Cells that attached overnight were washed with serum free media and incubated overnight in rIL-6 (200pg/ml) in serum free conditions. rIL-6 (200pg/ml) was also added to the Mito Stress Test media during the assay. Data show measurements from the Seahorse XF Anlayzer using the Mito Stress Test. The data are presented as mean ± SD of three independent experiments. Students t test or One-Way ANOVA were used for statistical analysis. *p<0.05, **p<0.01, ****p < 0.0001.

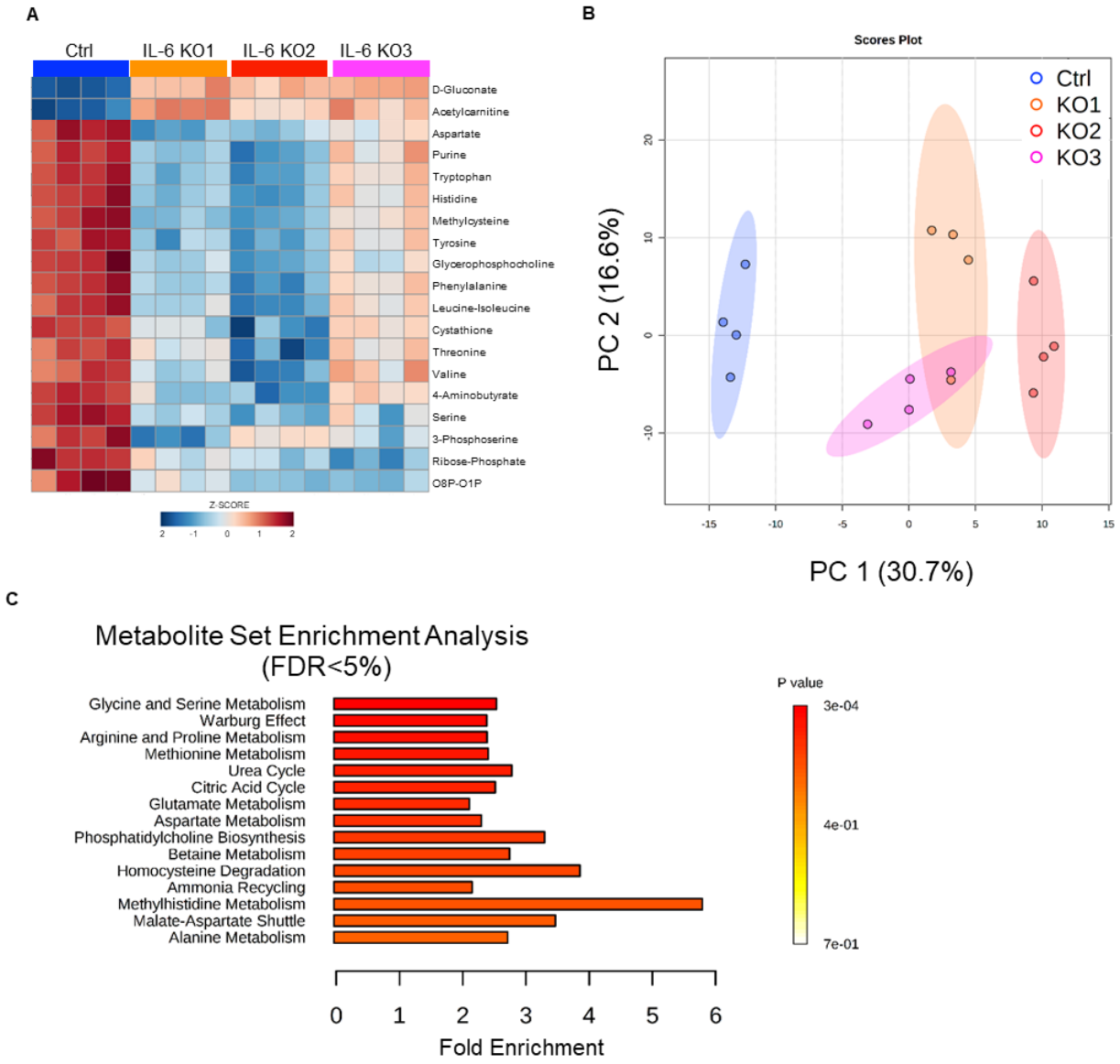

Fig. S3. IL-6 knockout shows a distinct metabolic signature. (*A*) Hierarchical clustering and heatmap showing the top 20 differential metabolites in three IL-6 knockout TSC2-deficient MEF clones compared to control. (*B*) Principal component analysis shows that the metabolism of the three IL-6 knockout clones is distinctive from control cells. (*C*) Metabolite Set Enrichment Analysis (MSEA) of differentially regulated metabolic pathways upon IL-6 knockout with false discovery rate (FDR) <5% identifies Glycine and Serine Metabolism as the most significantly regulated pathway. Heatmaps and MSEA were generated using MetaboAnalyst.

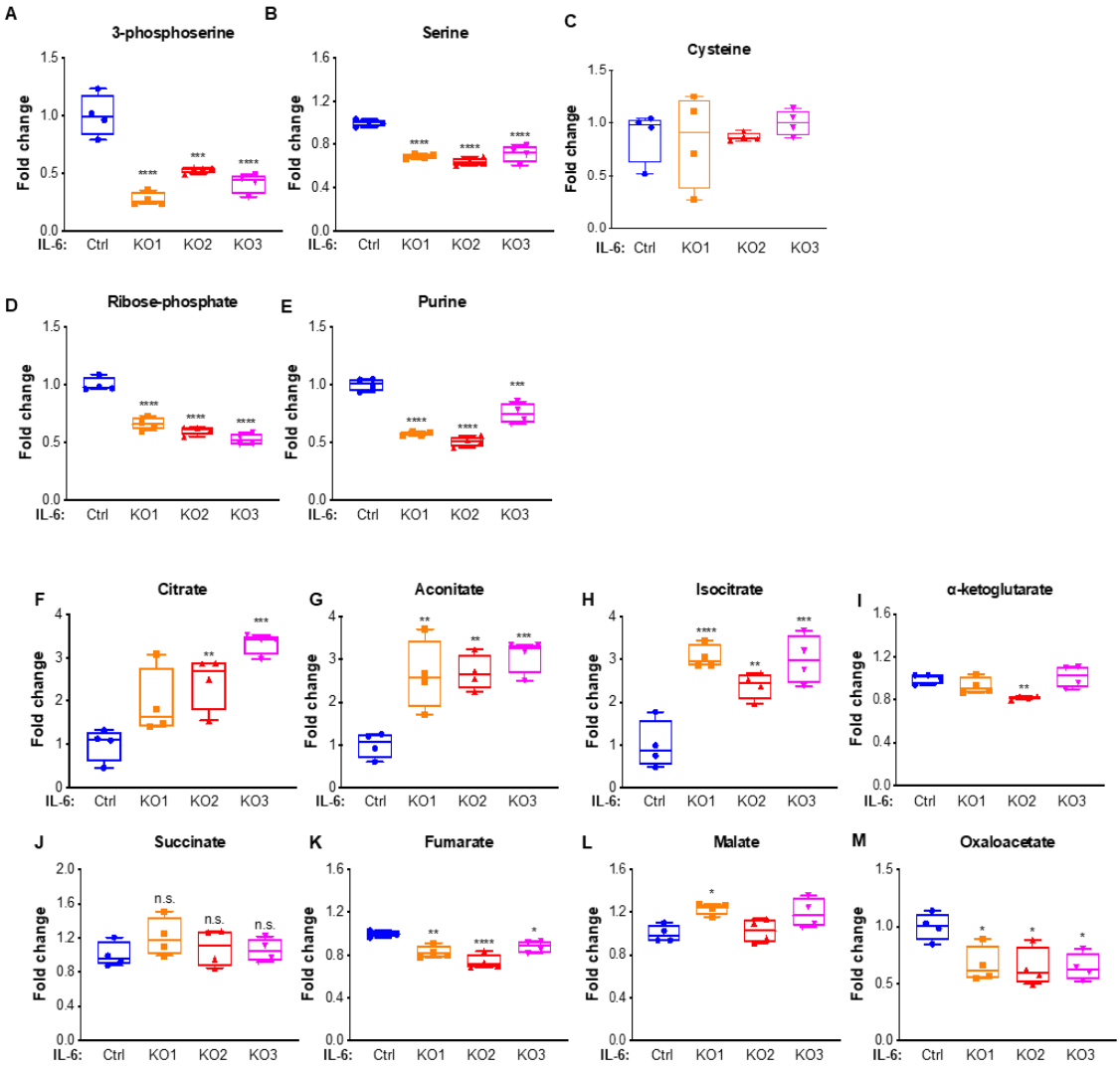

Fig. S4. IL-6 knockout decreases serine in TSC2-deficient cells. (*A-M*) Metabolites of *de novo* serine biosynthesis, pentose phosphate pathway and TCA cycle quantified by LC/MS were differentially regulated in IL-6 knockout, TSC2-deficient MEFs compared to controls. Data presented as individual values with box and whisker plot showing mean ± minimum and maximum value of four biological replicates. Statistical analysis was performed by One-Way ANOVA *p<0.05, **p<0.01, ***p<0.001, ****p<0.0001 as compared to control.

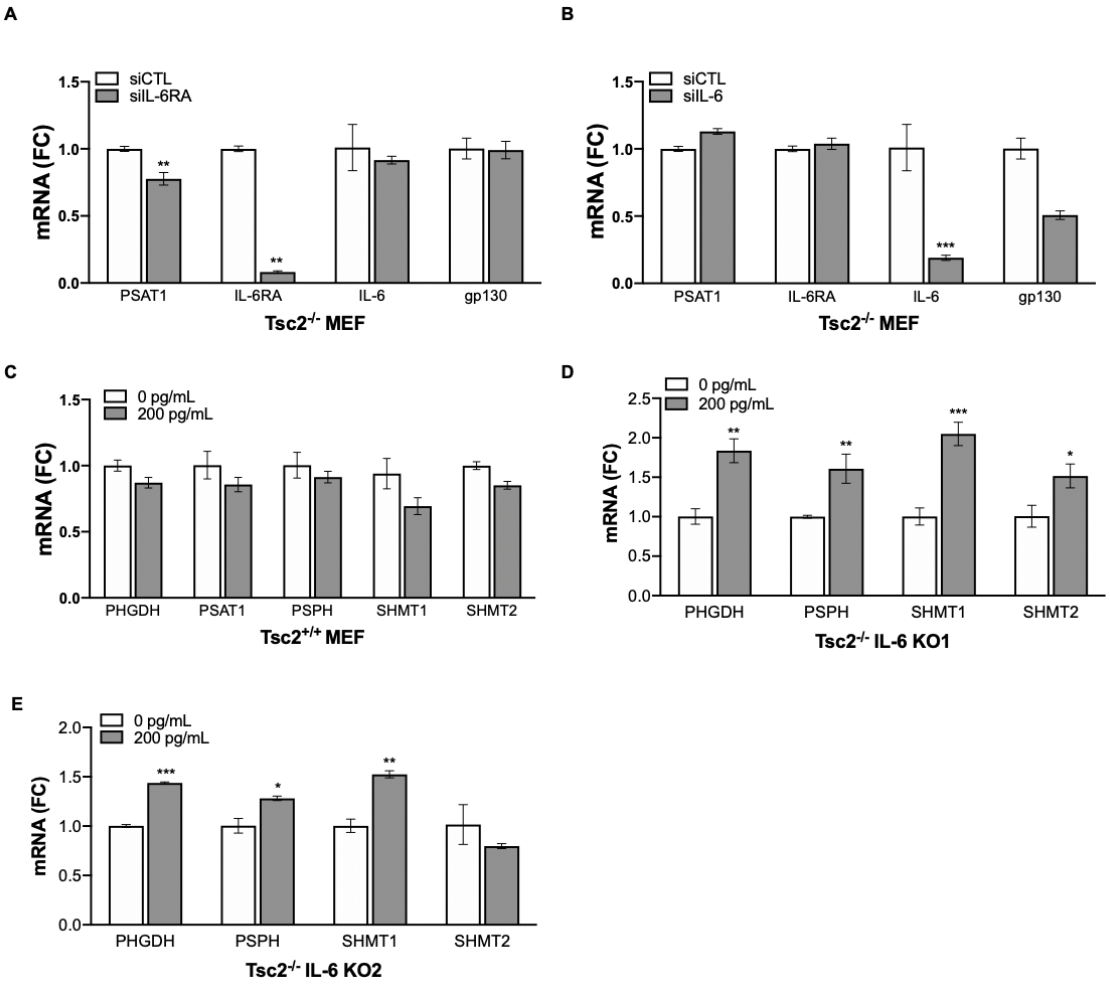

Fig. S5. IL-6 modulates serine biosynthesis genes in a TSC2-dependent manner. (*A*) IL-6 receptor knockdown using siRNA decreased *PSAT1* mRNA expression in TSC2-deficient cells. (*B*) *PSAT1* mRNA expression is unchanged by IL-6 knockdown using siRNA in TSC2-deficient cells. (*C*) Recombinant IL-6 (200pg/ml, 24h) has no impact on *de novo* serine biosynthesis genes in Tsc2 wildtype cells. (*D* and *E*) Recombinant IL-6 (200pg/ml, 24h) treatment of Tsc2-deficient IL-6 knockout cells increased the mRNA expression of serine biosynthesis genes. The data are presented as mean ± SD of three independent experiments. Student's t test was used for statistical analysis with * p<0.05, ** p<0.01, ****p*<0.001.

Supplementary Figure 6

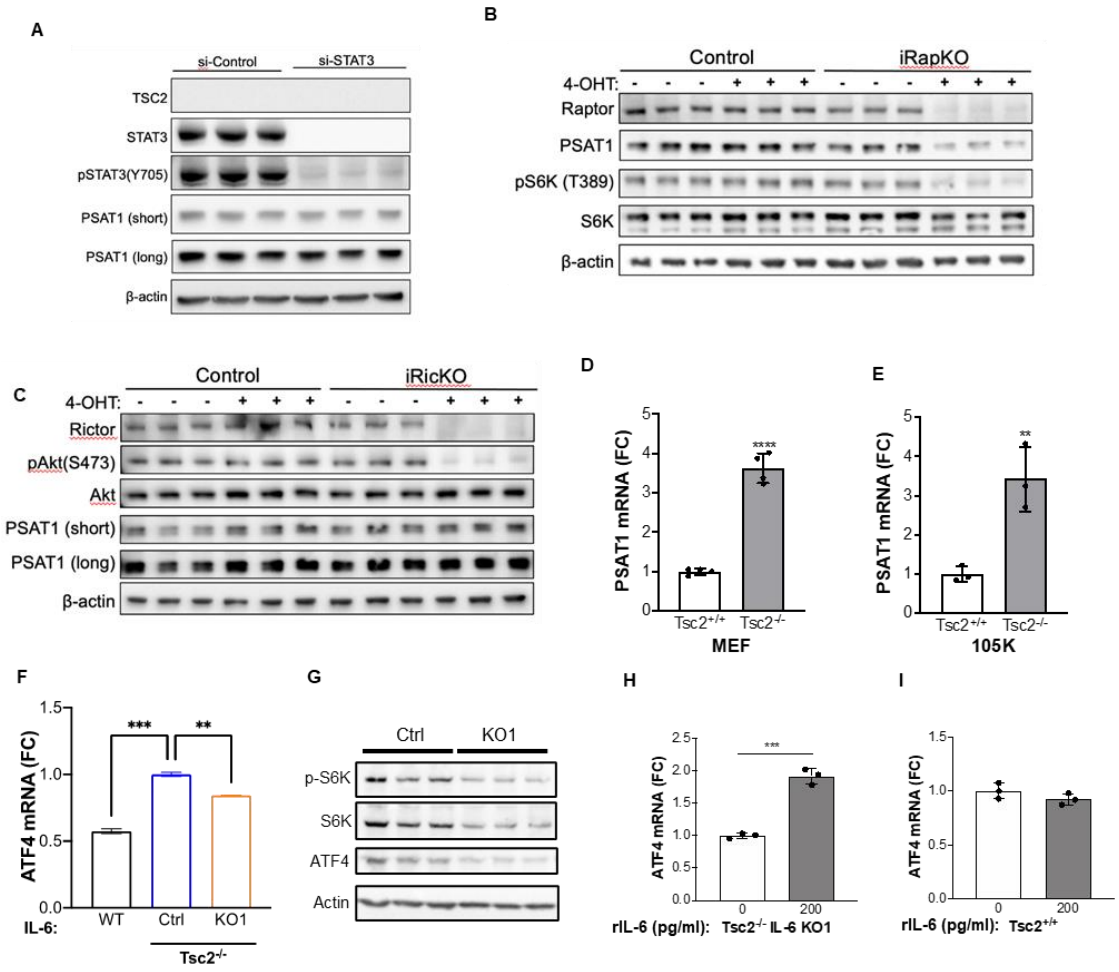

Fig. S6. PSAT1 is regulated in a STAT3-independent mTORC1-dependent manner. (*A*) Western blotting showing that inhibition of STAT3 using siRNA did not impact PSAT1 protein expression (72h siRNA, serum-free last 24h). (*B*) mTORC1 inhibition using inducible Raptor knockout cells decreased PSAT1 protein levels. (*C*) mTORC2 inhibition using inducible Rictor knockout had no impact on PSAT1 protein levels. (*D*) *PSAT1* mRNA levels are increased in TSC2-deficient MEFs compared to TSC2-expressing MEFs. (*E*) *PSAT1* mRNA levels are increased in TSC2-deficient mouse kidney cystadenoma 105K cells compared to TSC2 re-expressing cells. (*F*) *ATF4* mRNA levels are increased in TSC2-deficient cells compared to TSC2-expressing cells, while IL-6 knockout decreased *ATF4* expression. (G) Knockout of IL-6 inhibited phosphorylation of the mTORC1 target gene S6 kinase and the protein levels of ATF4. (*H*) Recombinant IL-6 (200pg/ml, 24h) increased the mRNA expression of *ATF4* in IL-6 knockout TSC2-deficient cells. (*I*) Recombinant IL-6 (200pg/ml, 24 h) did not impact the expression of *ATF4* in TSC2-expressing . Data are presented as mean ± SD of three independent experiments. Student's t test and One-Way ANOVA were used for statistical analysis with **p<0.01, ***p< 0.001, ****p<0.0001.

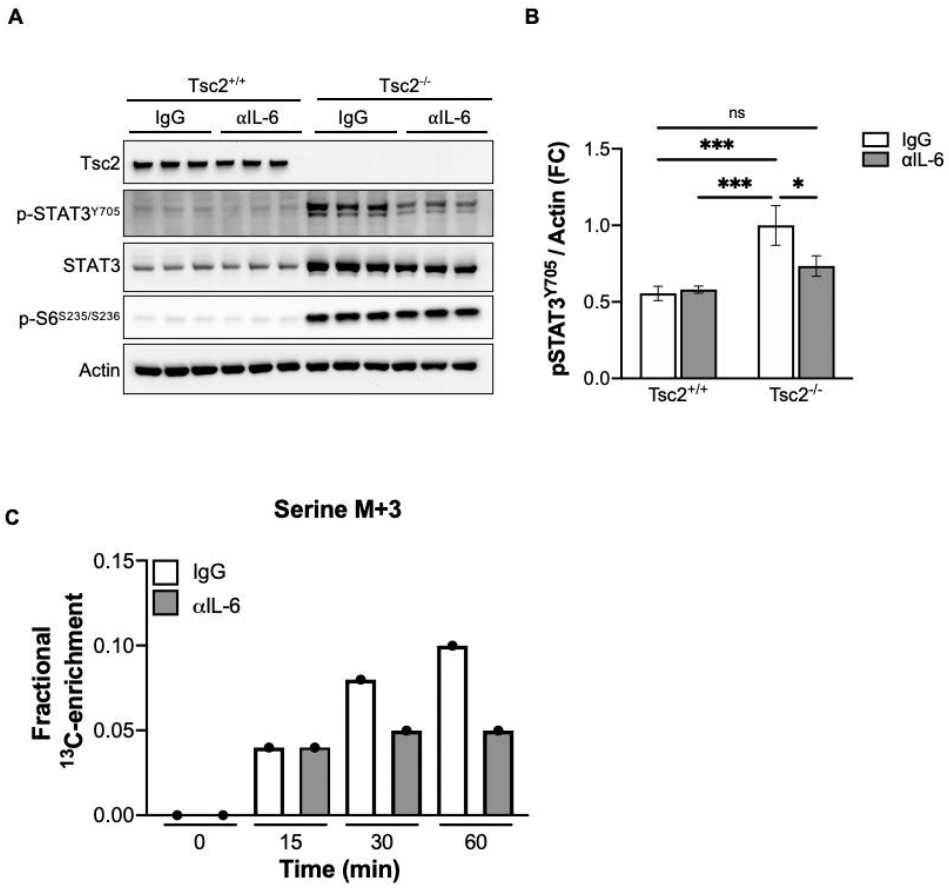

Fig. S7. αIL-6 antibody reduced STAT3 signaling and serine synthesis in TSC2-deficient cells. (*A*) Western blot and (*B*) densitometry show that αIL-6 antibody decreased phosphorylation of STAT3^{Y705} in TSC2-deficient cells (αIL-6 antibody, 10ug/ml, 24h). (*C*) U-^{13}C glucose tracing following αIL-6 antibody decreased M+3 serine levels compared to IgG antibody control (10ug/ml). Data in C are derived from a single biological replicate for each treatment condition and time point.

Supplementary Figure 8

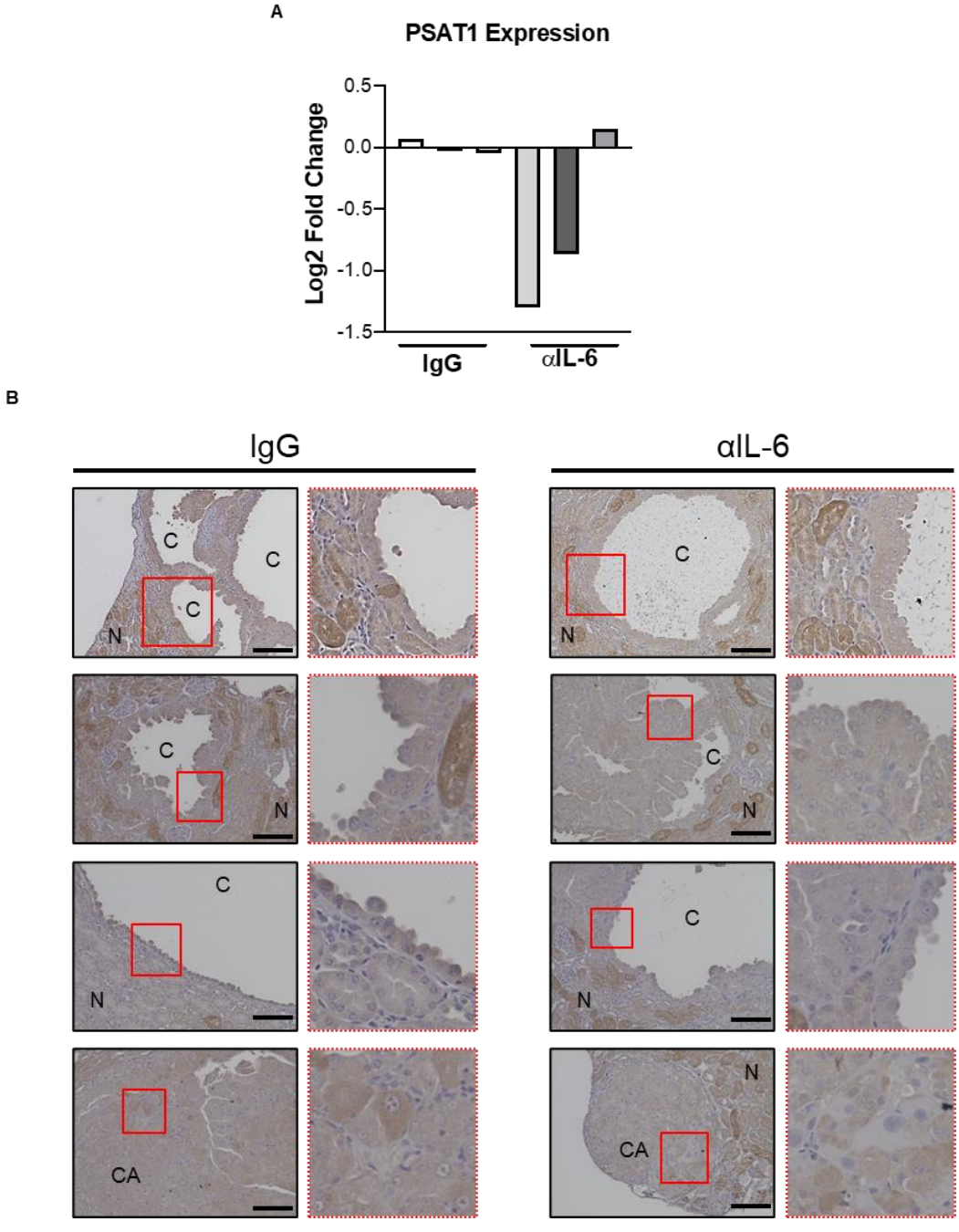

Fig. S8. PSAT1 expression is reduced in renal lesions of Tsc2$^{+/-}$ mice treated with αIL-6 antibody. (*A*) Semi-quantitative analysis of PSAT1 staining in three IgG and three αIL-6 antibody treated mice (200 ug/mouse, three times/week). (*B*) Representative PSAT1 staining from IgG treated kidney with outlined area in red enlarged in image (*Left column*). Representative PSAT1 staining from αIL-6 antibody kidney with outlined area in red enlarged in image (*Right column*). c-renal cyst, ca-cystadenoma, n-normal adjacent kidney, Scale bar = 100μm.

SI References

1. H. J. Liu *et al.*, Rapamycin-upregulated miR-29b promotes mTORC1-hyperactive cell growth in TSC2-deficient cells by downregulating tumor suppressor retinoic acid receptor beta (RARbeta). *Oncogene* **38**, 7367-7383 (2019).
2. M. Yuan, S. B. Breitkopf, X. Yang, J. M. Asara, A positive/negative ion-switching, targeted mass spectrometry-based metabolomics platform for bodily fluids, cells, and fresh and fixed tissue. *Nat Protoc* **7**, 872-881 (2012).
3. M. Yuan *et al.*, Ex vivo and in vivo stable isotope labelling of central carbon metabolism and related pathways with analysis by LC-MS/MS. *Nat Protoc* **14**, 313-330 (2019).